R-20

FINITE ELEMENT MODELING OF TWO-DIMENSIONAL TRANSMISSION LINE STRUCTURES USING A NEW ASYMPTOTIC BOUNDARY CONDITION

A. B. Kouki, A. Khebir, and R. Mittra

Department of Electrical & Computer Engineering
University of Illinois, Urbana, IL 61801

Abstract The finite element method is employed to study open, arbitrarily-configured two-dimensional transmission line structures in the quasi-TEM regime. An improved version of a previously developed asymptotic boundary condition(ABC) is used to truncate the open region. Results for two- and six-conductor configurations are presented to illustrate the superiority of this method over both the conventional approach where a perfectly conducting, enclosure is employed to truncate the FEM mesh, and the original ABC introduced previously by the authors. The results presented are of particular interest for estimating crosstalk and signal distortion in printed circuits.

I. Introduction

With the continuous advances in solid state devices technology in terms of both speed and size, a number of challenges are presented to the packaging engineer who has to accommodate a multitude of these devices on a limited real estate available on the circuit board. In the absence of reliable design tools, digital circuit packaging is carried out through a costly and lengthy trial and error process. Thus there exists a critical need for computer-aided design tools that are capable of predicting the electrical performance of a given package, e.g., crosstalk and signal distortion, in a reliable fashion. Understanding how printed circuit layouts can affect these quantities is essential for improved package designs. A first step toward achieving this goal entails the investigation of the signal integrity for a class of arbitrarily-configured two-dimensional transmission line structures.

A plethora of techniques are available in the literature for dealing with different transmission line configurations. However, a majority of these approaches are limited in their application to thin conducting etches and/or to structures containing dielectrics with planar interfaces. In contrast, the finite element method(FEM), can handle conductors with arbitrary cross-sections and arbitrarily inhomogeneous dielectrics. However, one drawback of FEM is that, in dealing with open region problems, it requires the introduction of an artificial outer boundary in order to limit the number of node points to a manageable size. The most common method for truncating an open region is to use of a perfect electric conductor as an external shield or to employ infinite elements for the same purpose [1-5]. Both of these approaches have major drawbacks and attempt was made in [6] to overcome some of them by applying an asymptotic boundary condition (ABC) on the outer boundary. The asymptotic boundary condition mimics, to a certain degree, the behavior of the field at infinity and is designed to yield accurate results in the interior region without the need for an exorbitantly large number of mesh points. Furthermore, the use of ABC does preserve the sparsity of the discretized finite element matrix and is, therefore, an attractive candidate for numerical applications. It was demonstrated in [6] that the asymptotic boundary condition consistently yields results that are more accurate than those obtainable with a perfectly conducting shield placed at the same location. However, in some situations, the accuracy obtained with the ABC presented in [6] was not adequate. This lack of accuracy is attributable to the fact that the asymptotic boundary condition operator used in [6] was based only on the use of the first two terms of the asymptotic representation of the solution to the Laplace equation.

In this paper, we attempt to circumvent this problem by deriving a higher-order asymptotic boundary condition. This boundary condition, unlike the one used in [6] which assumes that in the far region the solution can adequately be represented by the first two terms of the series, requires that the asymptotic representation be a combination of both the lower- and higher-order terms. As will be demonstrated later, a significant improvement in the

CH2848-0/90/0000-0717$01.00 © 1990 IEEE

finite element solution is achieved for both two- and six- conductor configurations when the higher-order ABC is used.

II. Derivation of the Higher-Order Asymptotic Boundary Condition

Consider the problem of N arbitrarily-shaped conductors embedded in a multilayered medium above a ground plane, shown in Figure 1. Let Ω_T denote the region exterior to the conductors and Γ_2 the outer boundary enclosing the truncated region. The potential u must satisfy Laplace's equation everywhere in Ω_T, the constant potential condition on the conductors, and the asymptotic boundary condition on the outer boundary Γ_2. Equivalently, the problem can be described in terms of the following equations:

$$\nabla\cdot(\varepsilon\nabla u) = 0 \text{ in } \Omega_T \qquad (1)$$

$$u = g_i \text{ on the } i^{th} \text{ conductor} \qquad (2)$$

$$B_m u = 0 \text{ on } \Gamma_2 \qquad (3)$$

where u is the electrostatic potential and B_m is the m^{th} order asymptotic boundary condition.

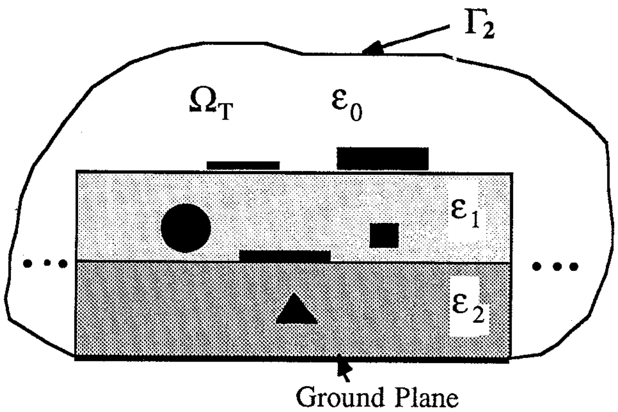

Figure 1. Multi-conductor transmission line in a multi-layered dielectric region above a ground plane.

In previous work [6], the asymptotic boundary condition was based on the first two terms of the asymptotic representation of the general solution to Laplace's equation. In this work, we suggest the following asymptotic form for the potential u

$$u = \frac{a_{n1}}{\rho^{n1}}\cos n_1\phi + \frac{a_{n2}}{\rho^{n2}}\cos n_2\phi + \frac{a_{n3}}{\rho^{n3}}\cos n_3\phi + \ldots \qquad (4)$$

with $n_1 < n_2 < n_3$. From (4), we can see that

$$\frac{\partial u}{\partial \rho} + \frac{n_1 u}{\rho} = \frac{a_{n2}}{\rho^{n2+1}}\cos n_2\phi(n_1-n_2) + \frac{a_{n3}}{\rho^{n3+1}}\cos n_3\phi(n_1-n_3) + \ldots \qquad (5)$$

Thus, we define the first order operator B_1 to be

$$B_1 u \equiv \frac{\partial u}{\partial \rho} + \frac{n_1 u}{\rho} = O\left(\frac{1}{\rho^{n2+1}}\right) \qquad (6)$$

Similarly, the second and third order operators can be expressed as

$$B_2 u \equiv \left(\frac{\partial}{\partial \rho} + \frac{n_2+1}{\rho}\right)\left(\frac{\partial}{\partial \rho} + \frac{n_1}{\rho}\right)u \qquad (7)$$

$$B_3 u \equiv \left(\frac{\partial}{\partial \rho} + (n_3+2)\frac{1}{\rho}\right)\left(\frac{\partial}{\partial \rho} + (n_2+1)\frac{1}{\rho}\right)\left(\frac{\partial u}{\partial \rho} + n_1\frac{u}{\rho}\right) \qquad (8)$$

For the finite element scheme formulation employed in this work, it is more desirable to have an access to the asymptotic representation for the normal derivative of u instead of the boundary condition operators derived above. To this end, we combine the B_3 operator in (8) and make use of the Laplace's equation to trade the second-order derivative in ρ, viz., $u_{\rho\rho}$, for the second-order angular derivative, $u_{\phi\phi}$. Then, by following the procedure described in [6], we can obtain the following expression for the normal derivative u_n in the local coordinate system (t,n), where t and n are the tangent and normal, respectively, to the triangular edge lying on the outer boundary Γ_2.

$$\frac{\partial u}{\partial n} = \bar{\alpha}(n_1,n_2,n_3,\rho)u + \bar{\gamma}u_t + \bar{\beta}(n_1,n_2,n_3,\rho)u_{tt} \qquad (9)$$

In the above equation u_t and u_{tt} are the first- and second-order tangential derivatives, respectively, and

$$\bar{\alpha}(n_1,n_2,n_3,\rho) = -(x_o\sin\theta_o - y_o\cos\theta_o)\frac{n_1n_2n_3}{\rho^2(n_1n_2+n_1n_3+n_2n_3)} \qquad (10)$$

$$\bar{\beta}(n_1,n_2,n_3,\rho) = (x_o\sin\theta_o - y_o\cos\theta_o)^3\frac{n_1+n_2+n_3}{\rho^2(n_1n_2+n_1n_3+n_2n_3)} \qquad (11)$$

$$\bar{\gamma} = \frac{1}{\rho^2}\left(-t(x_o\sin\theta_o - y_o\cos\theta_o) + \frac{1}{2}\sin 2\theta_o(y_o^2 - x_o^2) + x_o y_o\cos 2\theta_o\right) \qquad (12)$$

where θ_o, x_o, y_o, and t are as shown in Figure 2. More details on the implementation of (9) in the finite element scheme can be found in [6].

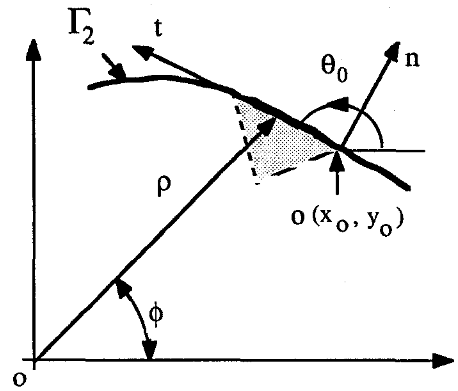

Figure 2. A triangular element residing on the outer boundary and its local coordinates.

III. Numerical Results

A. Two conductors

Consider the two coupled microstrips shown in Figure 3. The higher-order asymptotic boundary condition operator given by (9) was applied on a rectangular outer boundary. Choosing {1, 2, 4} for the set $\{n_1, n_2, n_3\}$, the finite element problem was solved for the electrostatic potential u and the capacitance matrix was computed. Table 1 shows the capacitance matrix values for the same problem that have been published elsewhere [7], together with those obtained by using a p.e.c. shield, the asymptotic boundary condition (the method of [6]), and the higher-order asymptotic boundary condition (present method). As Table 1 indicates, while both the present method and the simple asymptotic boundary condition yield more accurate results than those obtainable with a perfectly conducting shield placed at the same location, the higher-order asymptotic boundary condition results compare more favorably with the published work based on an integral equation technique.

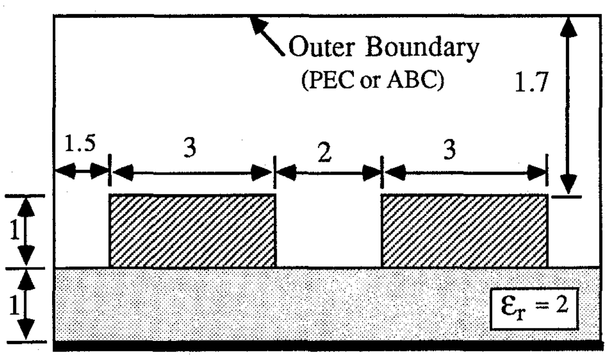

Figure 3. Coupled microstrips with rectangular outer boundary

B. Six conductors

Consider the six-conductor system shown in Figure 4. There are no published results for this configuration; however, we have compared our results with those derived by using the computer program developed by Harms *et al.* [8], which uses an integral equation formulation in the spectral domain followed by an iterative method of solution. For this configuration, although the simple ABC of [6] yields more accurate results than those obtainable with a perfectly conducting shield placed at the same location, the error in the capacitance matrix is noticeable, especially for the off-diagonal terms. Again the higher-order asymptotic boundary condition operator given by (6) was applied on a conformable rectangular outer boundary with a choice of the set $\{n_1, n_2, n_3\}$ to be equal to {1, 5, 10}. As Table 2 indicates, the higher-order asymptotic boundary condition yields a significant improvement over the simple asymptotic boundary condition, especially for the off-diagonal terms of the capacitance matrix.

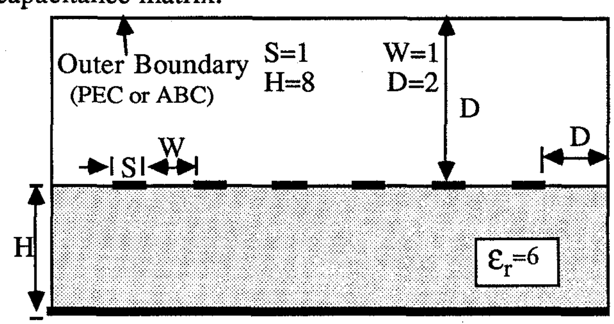

Figure 4. Six-conductor geometry.

Clearly, the improvements brought about by the higher-order asymptotic boundary condition are a direct consequence of its ability to incorporate lower- and higher-order terms through the choice of the set $\{n_1, n_2, n_3\}$. Based on numerical investigations, it was determined that the optimal choice of the set $\{n_1, n_2, n_3\}$ is $\{1, \rho/2, \rho\}$ where ρ is the distance from the origin to the middle of the edge of the triangular element residing on the outer boundary (see Figure 2).

IV. Conclusions

Starting from the asymptotic representation of the general solution to Laplace's equation, we have derived a higher-order asymptotic boundary condition that combines both the lower- and higher-order terms for a circular outer boundary. This boundary condition was subsequently generalized to the case of an arbitrary outer boundary and applied to the case of a rectangular outer boundary. The

	Reference [7]	Shield	ABC	Higher Order ABC	Error Shield-[7]	Error ABC-[7]	Error HOABC-[7]
C(1,1)	0.92×10^{-10}	0.10×10^{-9}	0.92×10^{-10}	0.92×10^{-10}	18.3%	0.27%	0.06%
C(1,2)	-0.85×10^{-11}	-0.47×10^{-11}	-0.80×10^{-11}	$-.83 \times 10^{-11}$	44.5%	5.20%	1.48%
C(2,1)	-0.85×10^{-11}	-0.47×10^{-11}	-0.80×10^{-11}	$-.83 \times 10^{-11}$	44.5%	5.20%	1.48%
C(2,2)	0.92×10^{-10}	0.10×10^{-9}	0.92×10^{-10}	0.92×10^{-10}	18.3%	0.27%	0.06%

Table 1. Capacitance matrix for the coupled microstrips of Figure 3.

	Iterative [8]	Shield	ABC	Higher Order ABC	Error Shield-[8]	Error ABC-[8]	Error HOABC-[8]
C(1,1)	0.66×10^{-10}	0.84×10^{-10}	0.68×10^{-10}	0.66×10^{-10}	26.83%	2.620%	0.213%
C(1,2)	-0.27×10^{-10}	-0.26×10^{-10}	-0.31×10^{-10}	-0.29×10^{-10}	5.340%	13.05%	4.983%
C(1,3)	-0.54×10^{-11}	-0.37×10^{-11}	-0.60×10^{-11}	-0.56×10^{-11}	32.56%	9.240%	2.826%
C(1,4)	-0.20×10^{-11}	-0.11×10^{-11}	-0.22×10^{-11}	-0.19×10^{-11}	43.71%	8.320%	7.631%
C(1,5)	-0.99×10^{-12}	-0.45×10^{-12}	-0.10×10^{-11}	-0.79×10^{-12}	54.30%	0.840%	20.73%
C(1,6)	-0.70×10^{-12}	-0.18×10^{-12}	-0.60×10^{-12}	-0.44×10^{-12}	74.10%	14.52%	36.74%
C(2,2)	0.78×10^{-10}	0.87×10^{-10}	0.84×10^{-10}	0.80×10^{-10}	11.03%	7.480%	1.713%
C(2,3)	-0.25×10^{-10}	-0.26×10^{-10}	-0.28×10^{-10}	-0.26×10^{-10}	3.960%	11.10%	5.220%
C(2,4)	-0.46×10^{-11}	-0.38×10^{-11}	-0.48×10^{-11}	-0.46×10^{-11}	17.23%	4.740%	0.193%
C(2,5)	-0.17×10^{-11}	-0.12×10^{-11}	-0.18×10^{-11}	-0.15×10^{-11}	29.03%	4.610%	9.869%
C(2,6)	-0.99×10^{-12}	-0.45×10^{-12}	-0.10×10^{-11}	-0.79×10^{-12}	54.30%	0.920%	20.67%
C(3,3)	0.79×10^{-10}	0.87×10^{-10}	0.85×10^{-10}	0.81×10^{-10}	10.14%	7.680%	2.307%
C(3,4)	-0.25×10^{-10}	-0.26×10^{-10}	-0.28×10^{-10}	-0.26×10^{-10}	4.870%	10.91%	4.043%
C(3,5)	-0.46×10^{-11}	-0.38×10^{-11}	-0.48×10^{-11}	-0.46×10^{-11}	17.23%	4.750%	0.127%
C(3,6)	-0.20×10^{-11}	-0.11×10^{-11}	-0.22×10^{-11}	-0.19×10^{-11}	43.71%	8.410%	7.416%
C(4,4)	0.79×10^{-10}	0.87×10^{-10}	0.85×10^{-10}	0.81×10^{-10}	10.14%	7.680%	2.307%
C(4,5)	-0.25×10^{-10}	-0.26×10^{-10}	-0.28×10^{-10}	-0.26×10^{-10}	3.960%	11.10%	5.220%
C(4,6)	-0.54×10^{-11}	-0.37×10^{-11}	-0.60×10^{-11}	-0.56×10^{-11}	32.56%	9.310%	3.053%
C(5,5)	0.78×10^{-10}	0.87×10^{-10}	0.84×10^{-10}	0.80×10^{-10}	11.03%	7.480%	1.713%
C(5,6)	-0.27×10^{-10}	-0.26×10^{-10}	-0.31×10^{-10}	-0.29×10^{-10}	5.340%	13.08%	4.983%
C(6,6)	0.66×10^{-10}	0.84×10^{-10}	0.68×10^{-10}	0.66×10^{-10}	26.83%	2.550%	0.328%

Table 2. Capacitance matrix (upper half) for the six-condutor structure of Figure 4.

numerical results for two- and six-conductor configurations demonstrated that the use of the higher-order asymptotic boundary condition results in a significant improvement over the simple asymptotic boundary condition employed in a previous work.

References

[1] Z. Pantic and R. Mittra, "Quasi-TEM analysis of microwave transmission lines in multilayered dielectric media," *IEEE Trans. Microwave Theory Tech.*, vol. MTT-32, pp. 705-710, July 1984.

[2] S. P. Castillo, "Electromagnetic modeling of high-speed digital circuits," Ph.D. dissertation, University of Illinois, Urbana, IL, 1987.

[3] Z. Pantic and R. Mittra, "Quasi-TEM analysis of microwave transmission lines by the finite-element method," *IEEE Trans. Microwave Theory Tech.*, vol. MTT-34, pp. 1096-1103, Nov. 1986.

[4] Z. Pantic and R. Mittra, "Finite element matrices for loss calculation in quasi-TEM analysis of transmission lines," *Microwave and Opt. Tech. Letters*, vol. 1, pp. 142-146, June 1988.

[5] M. Ikeuchi, H. Sawami, and H. Niki, "Analysis of open-type dielectric waveguides by the finite-element iterative method," *IEEE Trans. Microwave Theory Tech.*, vol. MTT-29, pp. 243-239, Mar. 1981.

[6] A. Khebir, A. B. Kouki, and R. Mittra, " Absorbing boundary condition for quasi-TEM analysis of microwave transmission lines via the finite element method", *Jour. of Electrom. Waves and Applicat.*, vol. 4, no. 2, 1990.

[7] W. T. Weeks, "Calculation of coefficients of capacitance of multiconductor transmission lines in the presence of a dielectric interface," *IEEE Trans. Microwave Theory Tech.*, vol. MTT-18, pp. 35-43, Jan. 1970.

[8] P. H. Harms, C. H. Chan, and R. Mittra, "Modeling of planar transmission line structures for digital circuit applications," *AEU* 43, pp. 245-250, 1989.